

Extension of the Brinkman-Rice picture and the Mott transition*

Hyun-Tak Kim**

Telecom. Basic Research Lab., ETRI, Taejeon 305-350, Korea

In order to explain the metal-Mott-insulator transition, the Brinkman-Rice (BR) picture is extended. In the case of less than one as well as one electron per atom, the on-site Coulomb repulsion is given by $U = \kappa\rho^2 U_c$ by averaging the electron charge per atom over all atomic sites, where κ is the correlation strength of U , ρ is the band filling factor, and U_c is the critical on-site Coulomb energy. The effective mass of a quasiparticle is found to be $\frac{m^*}{m} = \frac{1}{1-\kappa^2\rho^4}$ for $0 < \kappa\rho^2 < 1$ and seems to follow the heat capacity data of $\text{Sr}_{1-x}\text{La}_x\text{TiO}_3$ and $\text{YBa}_2\text{Cu}_3\text{O}_{7-\delta}$ at $\kappa = 1$ and $0 < \kappa\rho^2 < 1$. The Mott transition of the first order occurs at $\kappa\rho^2 = 1$ and a band-type metal-insulator transition takes place at $\kappa\rho^2 = 0$. This Mott transition is compared with that in the $d = \infty$ Hubbard model. The effective mass for 2D-DOS instead of the vHs can be used for the mechanism of high T_c superconductivity.

PACS number(s): 71.27.+a, 71.30.+h, 74.20.Mn, 74.20.Fg

Although several theoretical studies have been performed to reveal the mechanism of the metal-insulator transition (MIT),¹⁻⁴ the Mott MIT (called "Mott transition") in 3d transition-metal oxides including strongly correlated high- T_c superconductors still remains to be clarified.^{5,6} In particular, the effective mass near the Mott transition has attracted special attention because it is related to both the mechanism of the MIT and the two-dimensional density of states (2D-DOS). The latter offers a clue to explain the mechanism of high- T_c superconductivity.

In this paper, we build an extended BR picture with a generalized effective mass depending on the carrier density, which reduces to the BR picture in the case of one electron per atom, and apply it to experimental data of $\text{Sr}_{1-x}\text{La}_x\text{TiO}_3$ and YBCO.

In strongly correlated metals with one electron per atom, the on-site Coulomb repulsion U is always assumed as given. However, in real metallic crystals, in which the number of electrons n is less than the number of atoms m , U is determined not uniquely but instead by probability. In the case when $n = m$, the existence probability ($P = n/m = \rho = \rho_\uparrow + \rho_\downarrow$, "the band filling factor") of electrons on nearest neighbour sites is one. The on-site Coulomb interaction of two electrons in the conduction band is given by $U = U' \equiv \frac{e^2}{r}$. In the case when $n < m$, $P < 1$ and the on-site charge is $e' = eP$ (or $e'/e = P$), when averaged over sites. Then, the Coulomb energy is given by $U = P^2 U'$. U' does not necessarily agree with the critical value $U_c = 8|\bar{\epsilon}|$ of the interaction in the BR picture.¹ The Coulomb repulsion is thus given by

$$U = P^2 U' = \rho^2 U', \quad (1)$$

$$U' = \kappa U_c, \quad (2)$$

$$U = \kappa\rho^2 U_c, \quad (3)$$

where $0 < \rho \leq 1$, while $0 < \kappa \leq 1$ is the correlation strength. In the case of $\kappa \neq 1$ and $\rho = 1$ ($\rho_\uparrow = \rho_\downarrow = \frac{1}{2}$), U reduces to the correlation in the BR picture. In the case when $\kappa = 1$ and $\rho \neq 1$, U tends to U_c when the band approaches half filling. This indicates that having more

carriers in the conduction band increases the correlation, *vice versa*. For $\rho < 1$, U in metallic crystals is different from $U = U'$ in the $\rho = 1$ case and is not exactly defined, because U significantly varies from one site band to another. Therefore, U should be averaged over all atomic sites.

In order to use Eq. (3) in the BR picture, we should consider the conditions for applying U to the BR picture. In the Gutzwiller theory, $\bar{\nu}$ atoms are doubly occupied with a probability $\eta^{\bar{\nu}}$, where $0 < \eta < 1$.⁷ In the BR picture¹ at half filling $\rho = 1$ and $\rho_\uparrow = \rho_\downarrow = \frac{1}{2}$, $\eta = \bar{\nu}/(0.5 - \bar{\nu})$, and hence $0 < \bar{\nu} < 1/4$. For the lowest energy state, $\bar{\nu} = (1/4)(1 - \kappa)$ where $U/U_c = \kappa$, the above limits for $\bar{\nu}$ imply $0 < \kappa < 1$. When $\rho < 1$ and $\rho_\uparrow = \rho_\downarrow = \frac{1}{2}\rho$, the BR picture can be applied as well, with U averaged over all sites. Since the lowest energy state, $\bar{\nu} = (1/4)(1 - \kappa\rho^2)$ where $U/U_c = \kappa\rho^2$, is satisfied for $0 < \bar{\nu} < 1/4$, the condition $0 < \kappa\rho^2 < 1$ is reached. Thus the inverse of the discontinuity q in the BR picture,

$$\frac{1}{q} = \frac{m^*}{m} = \left(1 - \left(\frac{U}{U_c}\right)^2\right)^{-1}, \quad (4)$$

$$= \left(1 - \kappa^2\rho^4\right)^{-1}, \quad (5)$$

where m^* is the effective mass of a quasiparticle, is defined under the combined condition $0 < \kappa\rho^2 < 1$, although the separate conditions are $0 < \rho \leq 1$ and $0 < \kappa \leq 1$. Therefore, m^* increases without bound when $\kappa \rightarrow 1$, $\rho \rightarrow 1$. For $\kappa \neq 0$ and $\rho \rightarrow 0+$, m^* decreases and, finally, the correlation undergoes a (normal or band-type) MIT which differs from the Mott MIT exhibiting a first order transition. For $\rho = 1$, Eq. (5) reduces to the effective mass in the BR picture. At $\kappa\rho^2 = 1$, the MIT of the first order occurs and the state can be regarded as the paramagnetic insulating state because $\bar{\nu} = 0$. Eq. (5) is illustrated in Fig. 1 (a). In addition, the expectation value of the energy in the (paramagnetic) ground state is given by $\langle H \rangle_N = \bar{\epsilon}(1 - \kappa\rho^2)^2$. Here, the band energy $\bar{\epsilon} = \bar{\epsilon}_\uparrow + \bar{\epsilon}_\downarrow = 2\sum_{k < k_F} \epsilon_k < 0$ is the average energy without correlation and ϵ_k is the kinetic energy in the Hamiltonian in the BR picture¹, with the zero of energy

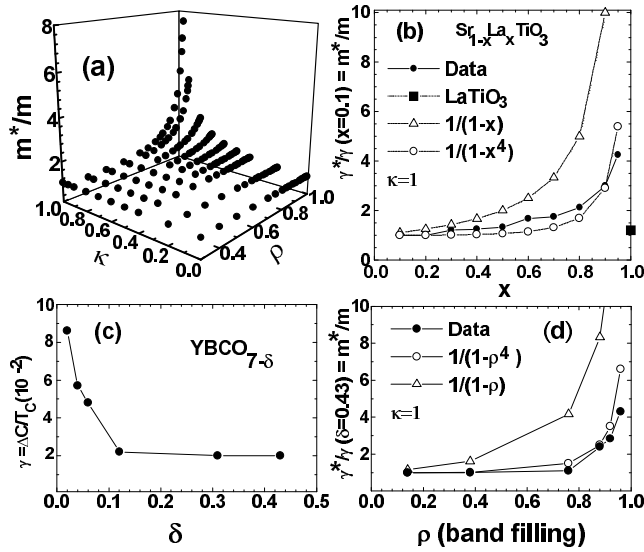


FIG. 1. (a) The effective mass, $\frac{m^*}{m} = \frac{1}{1-\kappa^2\rho^4}$. (b) Experimental data (\bullet) of the heat capacity for $\text{Sr}_{1-x}\text{La}_x\text{TiO}_3$ presented by Tokura⁵ and Kumagai⁶, and a comparison between $\frac{m^*}{m} = \frac{1}{1-x}$ calculated from the $t-J$ model (Δ) and $\frac{m^*}{m} = \frac{1}{1-x^4}$ (\circ). Here, ρ corresponds to x because the number of quasiparticles with x agrees with that of quasiparticles obtained from the Hall coefficient.⁵ Here, $\kappa=1$ and $0 < \kappa\rho^2 < 1$. (c) The heat-capacity coefficient ($\Delta c/T_c$) obtained by magnetic measurements for $\text{YBa}_2\text{Cu}_3\text{O}_{7-\delta}$ superconductors by Daümling.⁸ (d) In the cases $\delta=0$ and $\delta=0.45$, the band is assumed as full with $\rho=1$ and empty with $\rho=0$, respectively. Thus $\rho=1-\delta/0.45$. Here, $\kappa=1$ and $0 < \kappa\rho^2 < 1$.

chosen so that $\sum_k \epsilon_k = 0$. This picture may be called an extended BR picture with band filling.

On the other hand, in the $d = \infty$ Hubbard model², in which the width of the DOS $\rho(\omega)$ of the coherent part with a constant peak scale decreases with increasing U , the Mott transition occurs for the *minimum* number of quasiparticles, which number is an integral of $\rho(\omega)$ near $U = U_c$ to energies near $\omega = 0$. This is a marked difference from the BR picture in which the Mott transition occurs at $\rho=1$ (the *maximum* number of quasiparticles). The Mott transition in the $d = \infty$ Hubbard model can be regarded as the band-type MIT in the extended BR picture because of the decrease of the number of quasiparticles in the coherent part. In addition, the $t-J$ model³ and the Hubbard model⁴ on a square lattice predict critical behavior according to $m^*/m = 1/(1-x)$.

Eq. (5) is applied to the heat capacity data of the $\text{Sr}_{1-x}\text{La}_x\text{TiO}_3$, which is well known as a strongly correlated system. The number of quasiparticles determined by the Hall coefficient increases linearly with x up to at least $x=0.95$.^{5,6} The heat capacity in Fig. 3 of reference 5 is replotted, as shown in Fig. 1(b). Eq. (5) follows closely the heat capacity data in the case when $\kappa=1$. The first-order transition is found between $x=0.95$ and $x=1$. This

transition corresponds to the Mott MIT because $\kappa\rho^2 = 1$ in this picture, with $\rho = 1$ at LaTiO_3 and $\kappa = 1$ from the experimental result. Thus LaTiO_3 is a Mott insulator.

Eq. (5) is also applied to the specific heat data for YBCO measured by magnetic measurements by Daümling⁸. Eq. (5) seems to follow the data, as shown in Fig. 1(d). Although it is difficult to confirm whether YBCO at $\rho=1$ is a Mott insulator because the effective mass at $\rho=1$ is divergent, the divergence is regarded as a Mott transition.

We conclude from experimental data that the correlation strength is found to be $\kappa=1$, and that the presently proposed extended BR picture is better able to explain the Mott transition than Hubbard models. Finally, instead of the van Hove singularity (vHs), Eq. 5 should be used for 2D-DOS to describe the mechanism of high- T_c superconductivity.

I thank Mr. Nishio for valuable comments, and Prof. Tokura, Prof. Kumagai, and Dr. M. Daümling for permission to use experimental data in Fig. 1(b),(c).

* This is presented at 4PO1-3 of M2S-HTSC-VI Conference held at Huston at Feb. 20-25 of 2000 and will be published as the proceeding paper of 4PO1-3 in special volumes of Physica C (Elsevier Science B. V.) in 2000.

** kimht45@hotmail.com

¹ W. F. Brinkman and T. M. Rice, Phys. Rev. B **2**, 4302 (1970).

² X. Y. Zhang, M. J. Rozenberg, and G. Kotliar, Phys. Rev. Lett. **70**, 1666 (1993).

³ M. Kawakami and S. K. Yang, Phys. Rev. Lett. **65**, 2309 (1990).

⁴ N. Furukawa and M. Imada, J. Phys. Soc. Jpn. **60**, 3604 (1991).

⁵ Y. Tokura et al., Phys. Rev. Lett. **70**, 2126 (1993).

⁶ K. Kumagai et al., Phys. Rev. B **48**, 7636 (1993).

⁷ M. C. Gutzwiller, Phys. Rev. **137**, A1726 (1965).

⁸ Manfred Daümling, physica C **183**, 293 (1991).